Received: 9 January 2017 | Revised: 5 July 2017 | Accepted: 10 July 2017
DOI: 10.1002/gea.21663

RESEARCH ARTICLE

WILEY Geoarchaeology An International Journal

Evaluating ancient coastal wells as sea-level indicators from the coast of Israel

Reuven Vunsh[1] | Oren Tal[2] | Yoseph Yechieli[3,6] | Silas Dean[1] | Elad Levanon[3,4] | Dorit Sivan[1,5]

[1]Department of Maritime Civilizations, L. Charney School of Marine Sciences, University of Haifa, Mount Carmel, Israel
[2]Department of Archaeology and Ancient Near Eastern Cultures, Tel Aviv University, Tel Aviv, Israel
[3]Geological Survey of Israel, Israel
[4]Institute of Earth Sciences, The Hebrew University of Jerusalem, Jerusalem, Israel
[5]Leon Recanati Institute for Maritime Studies, University of Haifa, Mount Carmel, Israel
[6]Zuckerberg Center, Ben-Gurion University of the Negev, Sde Boker 8499000, Israel

Correspondence
Oren Tal, Department of Archaeology and Ancient Near Eastern Cultures, Tel Aviv University, Tel Aviv, Israel.
Email: orental@post.tau.ac.il

Scientific editing by Jamie Woodward

Abstract

This paper re-evaluates previous records and adds new data to the relative sea level (RSL; namely the sea level related to the level of the national terrestrial datum) reconstruction in Israel from the last 2400 years based on ancient coastal water wells. Different methods for obtaining the most accurate modern offset between coastal groundwater level and mean sea level are also tested, since this is a crucial component for using wells as reliable sea-level indicators in the Mediterranean and beyond. Very few, if any, sea-level studies outside of Israel use coastal wells as RSL indicators; refinements to the methods associated with this indicator type will facilitate their use in other regions. Coastal wells in the study are located within 200 m of the present-day coastline. The functional age range for the wells is based on site stratigraphy, artifacts, historical records, and the coastal water well typology. These archaeological indicators rely on finding the vertical offset between present-day coastal groundwater and sea level, and applying it to ancient times. The current study explores two methods to calculate accurate vertical offsets: a) modern averages of the upper aquifer groundwater elevation in the vicinity of ancient wells, which are calculated from 60 years of measurements by the Israeli Hydrological Service; and b) a hydrological model where groundwater elevation is a function of distance from the modern coastline. The model uses a simulation of the coastal aquifer with a two-dimensional, vertical cross-section. The modeled approach is found to be preferable. The results show that sea level in Roman times (1st century CE) was similar to present-day, slightly higher in the Byzantine period (4th to 7th centuries CE), and lower in part of the Early Islamic period (9th to 10th centuries CE). For the later Fatimid/Ayyubid and Crusader periods (11th to 13th centuries CE), RSL reaches its lowest elevations (of about −0.5 m) as previously found. Following these low levels, sea level rose going into the 18th and 19th centuries CE.

KEYWORDS
archaeology, coastal hydrological models, coastal water wells, sea level, water table

1 | INTRODUCTION

Archaeology is an important source for reconstructing past sea levels. The relationship of human-made structures to past sea level can be used when originally terrestrial sites are flooded or when coastal structures with a well-defined relation to the sea no longer function because of a change in sea level (Murray-Wallace & Woodroffe, 2014), as in the case of fish pools (ponds) or harbor installations. Archaeological sea-level indicators are discussed in detail by Morhange and Mariner in Shennan et al. (2014, and references therein). Sea-level researchers use the term sea-level index point (SLIP), which is defined as "reliable estimates of past changes in sea level relative to present, with quantified uncertainty terms" (Shennan et al., 2014, 8; used also by Vacchi et al., 2016). Sea-level indicators can be variously categorized, e.g., fixed sea-level indicators that always form a well-defined elevation to the land datum versus relational sea-level indicators that originally form at a wide range of elevations (Murray-Wallace & Woodroffe, 2014). In this study, we divide the archaeological indicators into primary and secondary groups. For obtaining past sea levels, primary indicators require only the artifact elevation at present and its original relations to sea level while it was functioning for human needs; fish pools are an example. Secondary indicators involve additional variables, such as the current water table and sea-level offsets required by coastal wells. Another distinction is the type of data point an indicator provides to sea-level reconstruction. While coastal water wells are index points that represent a fixed sea level with uncertainties for the age and past sea level, other types of artifacts like cisterns and coastal water mills, which are also secondary indicators, only provide upper limiting data points for sea level (see Methods below).

1.1 | Mediterranean sea-level curves based on archaeology

Archaeological research of paleo-sea level is well established in the Mediterranean, with the oldest Mediterranean record dating more than 20 ka at Cosquer Cave, France (Lambeck & Bard, 2000). For the Holocene, Flemming (1968) and Pirazzoli (1991) were the pioneers. Mediterranean studies in coastal archaeology, like those of Blackman (1982) and more recently those of Auriemma and Solinas (2009) concerning ancient harbors, and Blackman et al. (2014) on ship sheds in the Mediterranean, also comprise valuable sources for sea-level records. Combined observations and model predictions from the entire Mediterranean were presented by Anzidei et al. (2014), while Mediterranean-wide eustatic and glacial isostatic adjustment (GIA) models were produced by Lambeck and Purcell (2005) and Stocchi and Spada (2009).

Regional archaeological-based Holocene sea-level curves from other parts of the Mediterranean have also been recently published for the eastern Mediterranean by Sivan et al. (2001), for the Aegean by Lambeck (1995), Kosmas et al. (2012), Vött (2007) and Vacchi et al. (2014), for the central Mediterranean by Lambeck et al. (2004a; 2011) and Antonioli et al. (2009), and for the western Mediterranean by Pirazzoli (1976), Morhange et al. (2001) and Vacchi et al. (2016 and references therein).

For the last 2 – 3 ka, and especially the first half of the 1st millennium CE (or the Roman Period, as it is referred to archaeologically in the Mediterranean), there are numerous archaeological-based sea-level curves. For the eastern Mediterranean these include Sivan et al. (2004), Anzidei et al. (2011), Toker et al. (2012); such curves in the northwestern Mediterranean include Morhange et al. (2013) and Vacchi et al. (2016).

1.2 | The Israeli late Holocene sea-level curve based on archaeology

The Israeli (southern Levantine) Holocene relative sea-level (RSL) curve is based mainly on archaeological indicators, which are unequally distributed chronologically. Observations are complemented by GIA model predictions (Lambeck & Purcell, 2005; Sivan et al., 2001; Toker et al., 2012). These models produce different results when applied to the Israeli coast. The disagreement between models is another reason why empirical, carefully vetted archaeological indicators of sea level are important, since they provide a solid basis by which to evaluate and refine the parameters of model predictions.

According to the observational data, the sea reached its present level (with an uncertainty of about 1 m) along the coast of Israel between 4000 and 3600 years ago (Porat, Sivan, & Zviely, 2008; Sivan et al., 2001) with subsequent fluctuations. In the last 2000 years, archaeological observations indicate relative stability; with slightly lower levels rising almost to present elevation in the beginning of the 1st millennium CE (early Roman period). Since then, fluctuations have mainly been below present level, with a significant drop around −0.50 m at the beginning of the 2nd millennium CE (late Fatimid and Crusader periods) as presented in Sivan et al. (2001; 2004) and Toker et al. (2012) using archaeological indications, and in Sisma-Ventura, Yam, and Shemesh (2014) with bioconstructions.

Unlike the early Holocene, for which archaeological sea-level observations derive from fully submerged Pre-Pottery Neolithic – Chalcolithic sites on the Carmel coast of Israel (Galili & Weinstein-Evron, 1985; Galili, Weinstein-Evron, & Ronen, 1988; 2005; Galili & Nir, 1993), the last 2500 years of archaeological observations are mainly from coastal sites like Dor (Raban, 1995), presented by Sneh and Klein (1984) and Raban and Galili (1985), Galili, Zviely, and Weinstein-Evron (2005), Toker et al. (2012), and most recently by Dean (2015). Coastal man-made structures that originally had a relation to sea level are also divided into groups based on various criteria (e.g., Flemming, Raban, & Goetschel, 1978; Galili & Sharvit, 1998). Sivan et al. (2001) divided archaeological indicators into coastal installations (like fish pools, flushing channels, etc.), coastal water wells, and shipwrecks, each with different assumed vertical uncertainties.

1.3 | Wells as sea-level indicators

The current research uses secondary archaeological sea-level indicators, mainly coastal water wells, which are up to 200 m landward of the present coastline, as a tool for reconstructing past sea level. The methodology of using coastal wells was first developed and presented by Y. Nir of the Geological Survey of Israel (SOI) (Nir, 1997; Nir & Eldar, 1986). Nir investigated the connection between coastal well base elevations, the groundwater level, and sea level. The earliest wells, indicating low levels in two periods from the last 2500 years, were presented in Nir and Eldar (1986). In that preliminary study, two wells out of seven were very close to the coastline (25 m from the sea): one in Mikhmoret (dated to the Persian period, about 2500 years ago) and the other in Yavne-Yam (Fig. 1) from the Hellenistic period (about 2300 years ago). The base elevations of these two early wells are −1.40 m and −0.70 m, respectively. Nir and Eldar (1986) used an average modern water-table elevation for comparison with the ancient water level, which was estimated to range between 0.50 and 0.70 m.

Later, Sivan et al. (2004) used 64 coastal wells from Caesarea (Fig. 1), dated to subsequent periods from the 1st century to the end of the 13th century CE, for obtaining continuous RSL records. The Caesarea study assumed that a) the wells operated year round and b) the minimum necessary water column in the well for operation in ancient times was around 0.30 – 0.40 m. This minimum well water level is derived from the height of vessels or jars used to draw water with minimum turbidity. In their study, Sivan et al. (2004) took continuous measurements of the modern water column in two wells at Caesarea over a period of three months, obtained an average of 0.80±0.14 m water-table elevation, which was considered the "offset" between the present average water table and the sea level. This modern "offset" was used for calculating past sea level. Based on these assumptions the following calculation is used: well bottom elevation plus 0.30 m minus

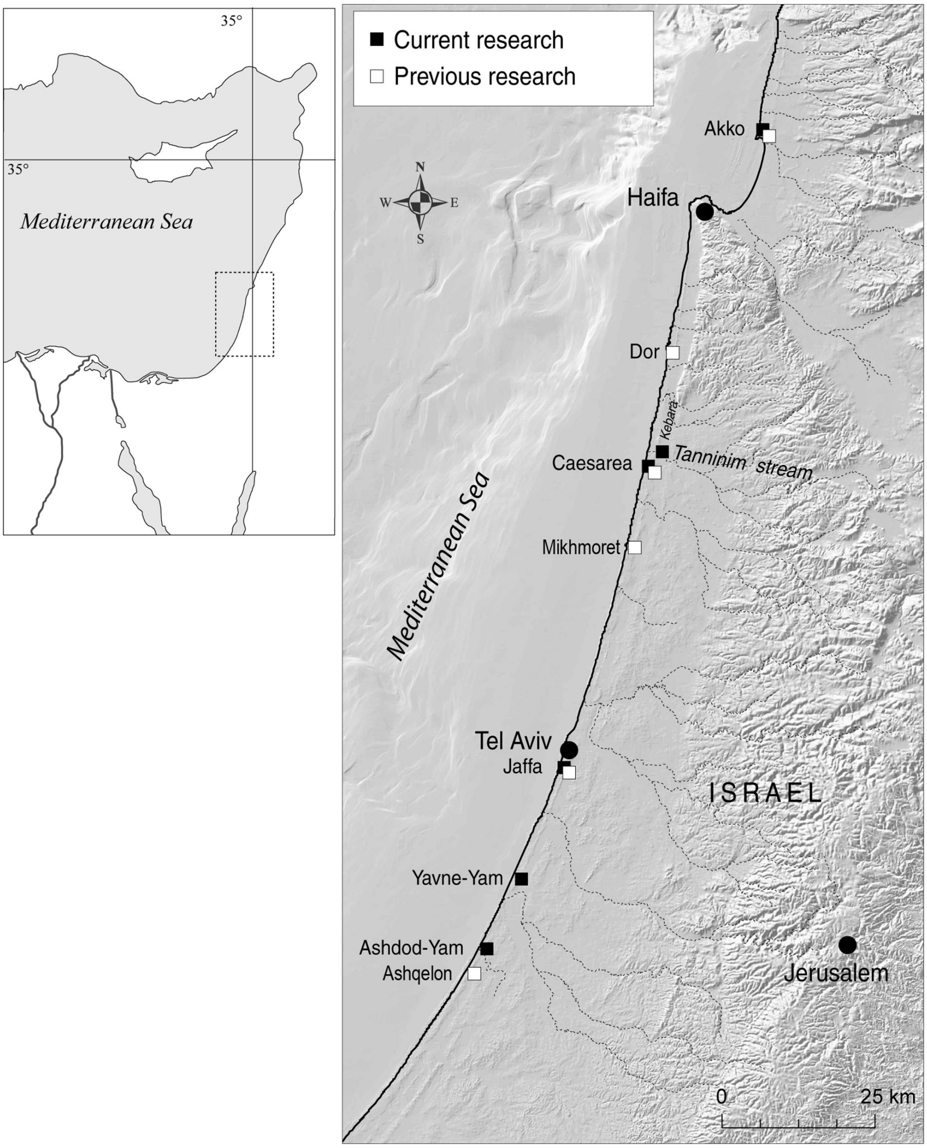

FIGURE 1 Left) Map of the eastern Mediterranean (study area in rectangle). Right) Ancient water well sites in Israel providing sea-level reconstructions

present-day offset between water table and sea level is equal to the sea level at the time of well construction.

The Caesarea water wells are mentioned in Auriemma and Solinas (2009) together with data from a few wells at the Etruscan site of Cerverti, Italy, dated from the 6th – 3rd centuries BCE. Their bottom is presently at −2.30 m to −2.60 m, indicating lower sea level, which was not calculated.

1.4 | Hydrological setting of the Israeli coastal aquifer

The Israeli coastal aquifer (Gaza Strip to Caesarea) is located along the eastern coast of the Mediterranean. Its length is 120 km, its width varies from 8 km in the north to about 20 km in the south, and its thickness varies from 200 m in the west to a few tens of meters in the east. The aquifer is composed mostly of sand, calcareous sandstone, siltstone, marine clay and shale of Pleistocene age (Issar, 1968), and lies above the Saqiye Group, which is composed of impermeable marine clay of Neogene age. In parts of the aquifer, local clay lenses divide it into several subaquifers, mainly in its western part. The relevant part in the current study is the upper phreatic portion of the aquifer, which is relatively homogenous and composed of sand and calcareous sandstone with almost no clay lenses. The general flow direction in the aquifer is from east to west, from the Judea Mountains toward the Mediterranean, based on the regional hydraulic gradient. This hydraulic gradient becomes steeper closer to the shoreline. The hydraulic conductivity of most of the aquifer is between 5 and 70 m/day (Issar, 1968; Lutzki and Shalev, 2010). The annual mean precipitation is ~500 mm/yr over most of the aquifer and the recharge to the aquifer is ~200 mm/yr.

The microtidal phenomenon in the Mediterranean has two daily cycles of high and low tide (Pugh, 1996). Along the eastern shore of the Mediterranean, the tidal amplitude varies from 0.5 m at spring tide to 0.1 m at neap tide. Tidal effect is much smaller in groundwater level than in the sea, as expected, depending mainly on the distance from the shoreline (Nielsen, 1990). These tide-induced oscillations can be up to 10 cm at distance of 70 m and diminish to less than 2 cm at 200 m (Levanon et al., 2013). Groundwater level is also affected by seasonal rise in sea level and by sea storms. Thus, the average sea level could be up to 0.3 m higher in the summer than in winter, affecting also groundwater level near the shoreline (Levanon et al., 2013). The effect of sea storms is mainly during the winter and it is more temporary. Another seasonal effect is due to higher recharge and reduced pumping in the winter, which could cause a higher level in the Israeli coastal aquifer of about 0.2 – 0.3 m. The latter effect is probably not significant in the near to shore area (< 200 m) and therefore less significant for the current study.

The coastal groundwater regime in Israel is divided into separate hydrological cells, some of which may have different hydrostatic pressure. The ancient water wells in the current research were drilled in parts of the aquifer with different lithological and hydrological conditions. The groundwater around Caesarea likely has higher recharge because it may have another source from the Judea Mountain aquifer, which is one of Israel's most important sources of fresh water (Dafny, Burg, & Gvirtzman, 2010). The aquifer is mainly discharging at Taninnim springs located at the northern tip of the basin (∼+3 m above sea level) several km to the north of the Caesarea area (Fig. 1). Some water may also flow from the Zikhron Ya'acov area to the sea around Caesarea (Kafri, 1967).

The coastal aquifer of the Western Galilee is thinner than the major coastal aquifer of Israel south of the Carmel coast and is fed mostly by water from the Judea aquifer in the Central Galilee (Kafri, 1970). This aquifer is probably shallower and poorer, e.g., in the area of Akko, relative to other locations of this research.

1.5 | Objectives

The current study assesses the accuracy of past RSL reconstructed from ancient coastal wells. Evaluating past sea level from wells relies on knowing the offset between modern water tables and sea level. This study aims to test different methods of calculating the offset for obtaining the most accurate results. Two methods were tested: a) calculating the average measured water-table elevations monitored in modern wells and b) using a model that calculates water-table elevations as a function of well distance from present-day shoreline. The study also presents the most up to date Israeli RSL record, based on re-evaluation of previous data and newly obtained measurements. Fulfilling these objectives will enable researchers to apply this proxy to other areas of the Mediterranean. Moreover, the current study shows how water wells in coastal sites are valuable sea-level indicators by using the best available modern water-table offsets.

2 | METHODS

2.1 | Excavations of ancient coastal water wells

All water wells in the current study (Fig. 1) are located within 200 m of the present-day coastline (Supplemental Table 1) and were previously excavated. In most cases, however, they were not exposed down to the well bottom since the water table rose as they were excavated. Since then, they were partially re-filled with dust and refuse, and had to be re-excavated and cleaned to their bottom course before being used as sea-level indicators. Construction of the wells involved digging a shaft to the water table and casing the shaft with elevated courses of worked building stones from top to bottom. In order to excavate these wells, an electric winch mounted on an elevated stand was used (Fig. 2a). A 200 L bag was hooked to the cable of the winch, filled with material accumulated inside the well, and then raised and emptied (Fig. 2b). Sherds and other indicative findings were separated and collected for further study and typological dating. The excavation stopped when the lowest course of stones was fully exposed (Fig. 2c).

2.2 | Measuring well bottom elevation

The cleared shafts were photographed, their diameters were recorded, and the depths of the lowest courses of stones were measured. Elevation measurements of the wells' upper courses were carried out by differential global positioning system (DGPS) relative to the Israeli ordnance datum (land datum). The accuracy of the vertical measurements by the DGPS varies between ±0.01 and ±0.05 m, depending on the distance of the site from the coastline/SOI benchmark and the number of real time kinematic terrestrial stations in the vicinity. The wells' depths from top to the base of bottom course were measured by a measuring tape. All well base elevations presented in Supplemental Table 1 are relative to the ordnance datum.

2.3 | Dating the operating periods of the RSL indicators

All of the new RSL indicators used in the current study are located in multi-period sites. The functioning age range of the indicators was determined according to previous excavations and then narrowed down according to typological characterization of new finds such as ceramic sherds and historical sources. Operating period of the wells was narrowed down to a single century (rather than a historical period) when possible.

2.4 | Modern water-table elevation

Reconstruction of ancient sea level depends on accurately determining the average modern offset between the present-day water-table elevation and current sea level following Sivan et al. (2004). In addition to continuous measurements in the ancient wells carried out previously (Table 1), two different methods of finding the most accurate offset were tested: a) calculating the decadal-scale average water-table elevations monitored in modern coastal wells near the surveyed archaeological sites (see: "new offset A" in Supplemental Table 1), and b) using a model to calculate water table as a function of the well distance from present-day shoreline (see; "new offset B" in Supplemental Table 1).

2.4.1 | Continuous measurements

Previous studies used short term (weeks or months), continuous measurements of water-table elevation in the studied wells compared to the national sea-level measurements made by the SOI (Table 1). This

FIGURE 2 Excavating a water well: a) an electric winch mounted on an elevated rail was used to remove accumulated debris in Yavne-Yam. b) a bag hooked to the winch cable filled with debris material removed from the well. c) the well at Yavne-Yam after excavation. d) Data logger at Ashdod-Yam [Color figure can be viewed at wileyonlinelibrary.com]

TABLE 1 Previous modern average water table used as offset

Site	Measurement location	Previous measured average water-table elevation (cm)	Measurement period	The closest sea tide-gauge location
Ashdod-Yam	Ashdod-Yam fortress, southern water well	31	20 days	Ashdod Marina
Jaffa	26 Nativ-Hamazalot St. water well	11	26 days	Tel Aviv Marina
Caesarea	Caesarea	80	90 days	Tel Aviv Marina
Akko	Hospitaller Compound, water well	19	180 days	Akko Marina

method was used in Caesarea (Sivan et al., 2004), Jaffa, Akko (Toker et al., 2012), and Ashdod-Yam (Vunsh, 2014).

In the current study, we put into test two Schlumberger microdiver pressure data-loggers in Ashdod-Yam, but since both of the sensors were placed in the well only for 20 days (one submerged at the bottom, while the other was hung at the top of the shaft, see Fig. 2d), we decided not to use their results in our calculations.

2.4.2 | Decadal averages of water-table measurements in modern wells

Water-table elevations from 21 modern water wells, taken for monitoring purposes, were collected. All wells are within 200 m from present coastline. The data were collected only from the upper subaquifer. The measurements were carried out periodically (with varying frequency) by the Israel Hydrological Service for the last 60 years. The modern water-table average elevations are presented in Table 2 and as "new offset A" in Supplemental Table 1. As shown later, these data points can include averages of wells with different distances to the shoreline, which can add an uncertainty of up to ±0.5 m to the RSL estimate if the distance is not taken into account.

2.4.3 | Model prediction of modern coastal water table as a function of the distance from present coastline

The groundwater level at different distances from the shoreline was estimated by simulation of the coastal aquifer, modified from the work of Levanon et al. (2017). The modeling was done with a two-dimensional, vertical cross-section using FeFlow, a finite-element simulator (Diersch, 2014) that solves the coupled variable density groundwater flow and solute transport equations.

The cross-section length is 1500 m, including 500 m seaward and 1000 m landward from the shoreline and its height is 120 m, of which 100 m is below mean sea level. The modeling was done for the general

TABLE 2 Average modern water-table elevations measured in water wells along the coast of Israel in the last few decades

Archaeological site	No. of modern wells in the vicinity of the archaeological site	Maximum distance from the archaeological site (km) to the south or to the north	Monitoring data points	Monitoring period	Average water-table elevations (m)
Ashdod-Yam	5	2	430	1960 – 1991	0.92
Yavne-Yam	3	2	800	1966 – 2006	0.98
Jaffa	5	5	500	1960 – 1988	0.97
Caesarea	7	2	1250	1957 – 2014	1.06
Akko	1	5	650	1959 – 2014	0.49

TABLE 3 Modern annual average of water-table elevation and hydraulic gradient (modeled and measured) as a function of the distance from the coastline. The difference between modeled and measured data is likely due to storm wave effects during the winter, which is not taken into account in the model. Numbers in brackets are the distances used for the gradient calculation

Distance from coastline (m)	Modeled[a]		Measured		
	Water level (m)	Hydraulic gradient (%)	Water level (m)	STDEV (m)	Hydraulic gradient (%)
20	0.24	1.2 (0 – 20)	0.3	0.29[b]	1.50 (0 – 20)
50	0.34	0.33 (50 – 20)	0.42	0.18	0.40 (50 – 20)
70	0.39	0.25 (70 – 50)	0.59	0.14	0.85 (70 – 50)
100	0.46	0.23 (100 – 70)	–	–	–
150	0.55	0.18 (150 – 100)	–	–	–
200	0.63	0.16 (200 – 150)	0.70	0.07	0.08 (200 – 70)

[a]Estimated by general simulation of the Israeli coastal aquifer (modified after Levanon et al., 2017).
[b]Water level 20 m from coastline was monitored only during winter (therefore its standard deviation is relatively high).

conditions of the Israeli coastal aquifer. For most accurate results, however, a similar process for each individual site with its specific, best-known hydrological parameters is advisable, and if possible, calibration with local field data of groundwater level and hydraulic conductivity (K). For the present study, K was taken to be 100 m/day, which is probably a reasonable value for the area near the shore that is built mostly of sand (Levanon et al., 2017). Porosity was estimated to be 0.3 (volume ratio with no units) for this sandy unit. At different distances from the shoreline along the coast, an average water level was taken to account for tidal effects. The groundwater levels at different distances were used as “new offset B” (Table 3 and Supplemental Table 1).

2.5 | Secondary indications obtaining sea-level constraints

Two more secondary archaeological indicators of RSL upper limiting constraints were checked: coastal cisterns and coastal dammed water mills.

2.5.1 | Coastal cisterns as upper RSL constraints

Plastered cisterns allowed storage of water collected by drainpipes and trenches. In the medieval and pre-modern periods, cisterns were often constructed in the vicinity of a water well, enabling the inhabitants to access fresh water when the well was depleted or in use. A well-and-cistern system was found at Ashdod-Yam and in the Mata family house and the International Conservation Center (ICC) building at Akko (Figs. 1 and 3). Cisterns were sealed using plaster applied in dry conditions only; the cistern floor elevation at time of construction therefore had to be at least ≥0.20 m above the local water-table level. Thus, cisterns function only as an upper limiting point for sea level.

2.5.2 | Coastal dammed water mills as upper RSL constraints

The use of coastal dammed watermills as a tool for constraining sea level was introduced in Vunsh (2014). Sluice gates positioned at the top of the Taninnim Dam controlled the flow of water accelerating down chutes, pipes, or channels, where it propelled vertical or horizontal turbines which rotated millstones and then flowed down to the sea (Figs. 1 and 4). Utilizing the full potential energy of the water means that turbines had to be placed as low as possible. However, the turbine base also had to be above downstream water elevation (close to sea level) in order to avoid hydrostatic resistance to rotation. This type of indicator is used only as an upper limiting data point for sea level.

2.6 | Dating and vertical errors of sea-index points

All index points include uncertainties for both chronological and vertical position. Most of the Caesarea wells from Sivan et al. (2004) and other wells used in the current study are dated within a range of up to 200 or 300 years solely by means of archaeological typology. Vertical errors for relative sea level are calculated from the root of the sum of the square of the component sources of error (see Hijma et al., 2015, 456). Attempt is made to approximate the 2σ error for each component. For wells, the component errors include 1) measurement

FIGURE 3 Cisterns: a) a plastered reservoir under the Ottoman-period Jazar Pecha Mosque, at Akko. b) Crusader-period cistern excavated on the site of the ICC in the Old City of Akko (by courtesy of D. Syon, Israel Antiquities Authority) [Color figure can be viewed at wileyonlinelibrary.com]

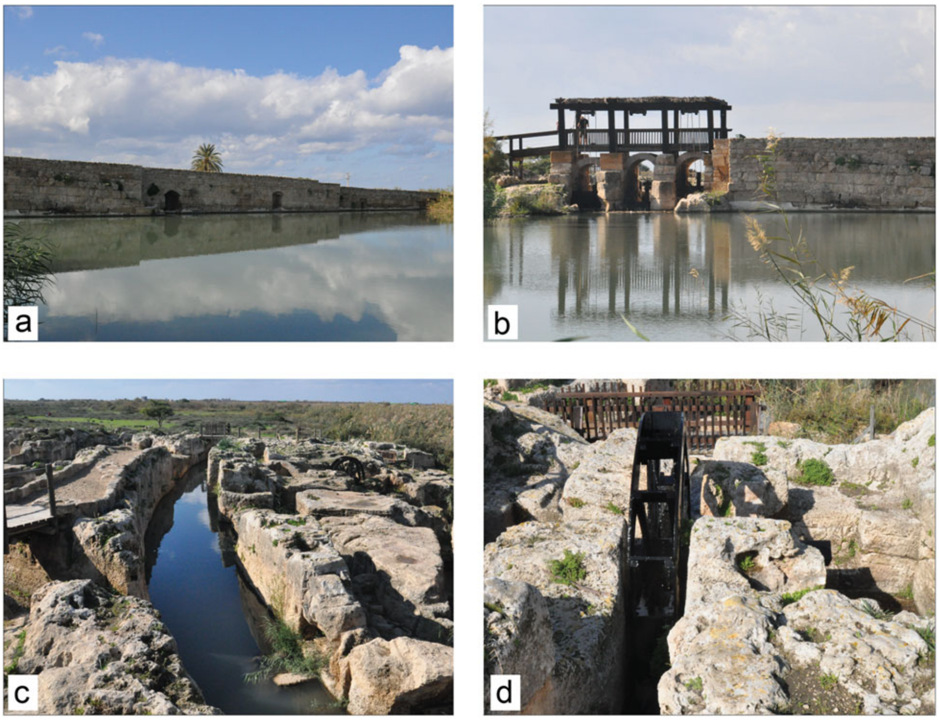

FIGURE 4 Taninnim stream dam and reservoir: a) the Byzantine western wall damming the channel and creating the artificial water reservoir; B) water outlets built in the dam; C) remains of one of the horizontal Ottoman-period waterwheel mills; d) reconstructed water mill shafts [Color figure can be viewed at wileyonlinelibrary.com]

error of the base elevation, 2) measurement error for the water level used to assess water-table elevations, 3) a range of permissible heights for the water column at the bottom of the well in which a class of drawing vessels could function, and 4) an uncertainty for the height of the water-table offset from sea level. In the current study, this last component is the 2σ of all measured water-table offsets at whichever of several distances (see Table 3) from shore most closely approximates the distance of the specified well from shore.

3 | RESULTS

Five water wells at Ashdod-Yam, Yavne-Yam, Jaffa, and two at Akko (Fig. 1 and Supplemental Table 1) were found suitable for this research and were therefore re-excavated and documented as SLIPs. The procedure and results of three of the excavations were recently published in preliminary form (Vunsh, Tal, & Sivan, 2013; 2014a; Vunsh et al., 2014b). An additional coastal well in Caesarea studied by Gleason et al.

(1998) is also included in the current study. Taninnim watermills and a cistern in Akko (Fig. 1) were successfully measured as upper constraints for past sea level.

3.1 | Coastal water wells base elevation

3.1.1 | Ashdod-Yam

A two-day excavation took place at the Ashdod-Yam fortress (Fig. 1) in September 2012, during which time the southern well shaft was completely cleared of modern debris. In December 2012, the tide gauges were placed inside the well for 20 days.

The well, about 1.10 m in diameter and 5.48 m deep, consists of 28 courses of sandstone (locally named *kurkar*) blocks, located about 80 m inland from the coastline. Two vertical slots at opposite sides, about 0.05 m deep and 0.10 m wide, run from top to bottom of the shaft. Flat slabs of conglomerated beach-rock were found at the bottom. The well base is at −0.28±0.10 m (Supplemental Table 1).

Initially, it was concluded that the well had been dug during the first phase of the fortress during the reign of the Umayyad Caliph ʿAbd al-Malik (685 – 705 CE) and supplied drinking water for inhabitants and livestock (Vunsh, Tal, & Sivan, 2013). Later, we considered re-dating the well to the Fatimid or Crusader period (10th to 12th centuries CE) given the existence of another well in the fortress that seems to better fit the courtyard's original Umayyad layout. As previous excavations at the site were unable to provide evidence for the construction of the well during the Umayyad period (Raphael, 2014), we favor the later date for its construction.

The uniformity of the shaft indicates that it had not been modified and kept the original base elevation. The longitudinal slots served as rails for supporting *antilya* jars whose lifting apparatus was mounted on marble columns. The beach-rock slabs were placed at the well base in order to improve water quality and to reduce sand turbidity. The water lifted from the well was then poured through a sand-settling pool and into the cistern located to the south.

The continuous measurements of the water level inside the well conducted for 20 days (Fig. 2d) showed that the groundwater level responds to tide cycles, with an average elevation of 0.316 m above simultaneously measured sea level (Table 1).

3.1.2 | Yavne-Yam

A one-day excavation of a well at this site took place on October 2012 in collaboration with the Director of the Yavne-Yam excavations M. Fischer of Tel Aviv University and assistance from Palmachim National Park staff (Fig. 1). Some 0.50 m of sand and stones were extracted until the bottom course was exposed.

The round well, about 1.50 m in diameter, is constructed of 43 kurkar block courses. The uniform shaft is about 7 m deep; its base elevation is at −0.02±0.10 m, and it is located some 50 m inland from the coastline. Conglomerated beach-rock paving was found at the bottom of the well (Vunsh, Tal, Sivan, & Fischer, 2014b).

The dating was based on two assemblages found inside the well in previous excavation seasons (Tal & Taxel, 2012). The earliest pottery from the lower assemblage indicates that the well had been dug during the 6th century CE, while the latest artifacts from the upper assemblage imply re-use of the shaft for dumping purposes in the early Islamic period, probably when the *ribat* (the Muslim coastal fortress) was founded during the reign of the Umayyad Caliph ʿAbd al-Malik (685 – 705 CE). The median value of the date estimated for the well is 550 CE, with an uncertainty range of ±50 years (Table 1). The uniformity of the shaft indicates that it had not been modified and retained the original base elevation. Beach-rock slabs were also used in this well to improve water quality and reduce turbidity.

3.1.3 | Jaffa

Only one well out of several surveyed in Jaffa for the current study produced relevant data: that within the Abu al-Afia restaurant (Fig. 1 and Table 1). The well was explored on November 2012. The shaft was found to be clear of obstructions and sediment.

The well, about 1.5 m in diameter and 10 m deep, consists of 36 sandstone block courses. Its base elevation is at +0.08±0.10 m and is located some 150 m inland from the coastline. There are pairs of opposed niches in every third course that served as an integrated ladder. The base support hoop behind the bottom course is made of iron. The uniform shaft extends to the well bottom (Vunsh, Tal, & Sivan, 2014a). At the time of our exploration, the bottom was merely damp though water had been observed during prior visits. The well is annexed to the Jerusalem Gate house constructed by the Ottoman governor Muhammad Abu-Nabut during the first decade of the 19th century. A photograph taken by Felix Bonfils in the 1870s shows the gatehouse entirely without the well or the covering (Arbel & Rauchberger, 2012). According to the photograph, iron hoop, architectural features, and remains of weaponry found inside the well, it was dug between 1890 and 1910.

3.1.4 | Caesarea

The promontory seaside palace in Caesarea (Fig. 1) was built by King Herod in two phases between 22 and 10 BCE. The building continued to serve as an imperial residence into the Byzantine era (Netzer, 1996). In the excavation season of 1994, a water well was discovered and cleared in the upper part of the palace. A total of 94 coins were found at the bottom of the well; 22 were identified and all were minted during the 4th century CE (Gleason et al., 1998). The well base elevation was measured using DGPS at 0.0±0.10 m (K. Gleason, personal communication). The finds inside the well indicate that it was dug and operated in the 4th century CE following a Byzantine renovation of the upper palace. The well age estimation is 340 CE, with an uncertainty of ±60 years (Supplemental Table 1). It is located some 20 m inland from the coastline.

3.1.5 | Akko

Two water wells were measured in Akko (Fig. 1) for the current study. On October 2012, the base of the Matta family well (Supplemental Table 1) was exposed by removing 300 kg of dirt and concrete using an electric winch and a sludge pump.

The Matta family well has a square section 1 × 1 m. The top 3 m of the 6.90 m vertical shaft is built of fossilized dune sandstone blocks, and the bottom section is cut into bedrock sandstone. There are pairs of niches carved in the shaft which enable climbing. The well was covered by a column base in a secondary use, and a round port had been cut in the center of the marble slab to enable drawing of water (Zach, 2007). The well base elevation is at 0±0.10 m (Supplemental Table 1). Based on architectural features, the location of the building and the history of the Christian family residing there, we conclude the well was dug during the rule of Dhaher al-Omar, when he encouraged Christians to re-settle Akko. The median value of the date estimated for the well is 1760 CE, with an uncertainty range of ±15 years. This well is located about 120 m from the coastline.

The ICC building (Supplemental Table 1) is a multiphase structure. It began as a fortified palace on the western edge of the Pisan quarter built during the Second Kingdom of Jerusalem. An Ottoman courtyard house covered it later and turned the structure into a main-hall house and a residential building in the Mandate period (Cocks, 2007). The well was discovered in hidden niches behind the wall during building renovation in 2009. The well base elevation is +0.16 m ±0.10 m (Supplemental Table 1). It was dated to the Crusader period with an estimated median date of 1251 CE ±50 years. The well is located about 50 m from the coastline.

3.2 | Cisterns

The only cistern excavated and used in the current research is in the ICC building in Akko. The cistern's base elevation is +0.77 m ±0.10 m (Supplemental Table 1). Paint and mortar residues on the cover stone indicate that the cistern was dug in the Crusader period during the Second Kingdom of Jerusalem (Zach, 2007). The estimated median date is 1251 CE, with an uncertainty range of ±50 years.

3.3 | The Taninnim dam watermills

The watermills are located along the southern wall of Caesarea's low aqueduct dam, about 1 km east of the shoreline (Figs. 1, 4c and 4d). The watermills were discovered in 1991 and were excavated by the Israel Antiquity Authority. Later, they were restored and reconstructed (Sa'id, 2002; Sa'id & Ad, 2004). The excavation revealed that a catchment area of about 6 km^2 was dammed during the Byzantine period by the construction of two walls up to 7 m in height: a western wall along the coastal ridge (Figs. 4a and 4b), and a northern one located to the northeast. Six inlet channels for vertical Byzantine water wheels were cut into the bedrock south of the dam. Remains of six horizontal Ottoman waterwheel mills were found along the dam. These water mills were originally constructed with nozzles at the bottom of shafts fitted to inlets located 5.50 m above mean sea level (MSL) as measured in the current study. A jet powered by the water column inside the shaft would flow from each nozzle to spin a bucket wheel. Four watermills were later refitted and the shafts were blocked and replaced by water chutes with inlets located +4.10 m (Dray, 2011). In 1924, the coastal ridge was breached in order to drain the malarial Kebara swamps (Fig. 1) and the watermills went out of use.

TABLE 4 Caesarea groundwater levels segmented by decade

Years of measurement	Average groundwater level (m)	Number of readings
1957 – 1960	1.03	135
1961 – 1970	1.09	334
1971 – 1980	1.08	264
1981 – 1990	0.93	230
1991 – 2000	1.13	133
2001 – 2010	1.05	144
2011 – 2014	1.16	44

The base elevations of the two Byzantine channels are at +1.02 m and +1.05 m (Supplemental Table 1), while the two early Ottoman outlet channels are at +0.55 m and +0.51 m. The re-use of the dam and the building of new watermills could have occurred between 1525 and 1825 CE under a strong central government. The median date for the early Ottoman watermills is 1675 CE ±150 years. The four late Ottoman channels are at elevations between +1.24 m and +1.27 m (Supplemental Table 1). These watermills were constructed in the 19th century after the dam wall was renovated and the water inlets were lowered to +3.5 m. Photographs from the beginning of the 20th century indicate that the mills were still functioning (Dray, 2011). The median date for the late Ottoman watermills is 1870 CE ±30 years.

3.4 | Calculation of modern water-table offset compared to sea level

The current study uses the transfer function proposed in Sivan et al. (2004): well base elevation plus 0.30 m (the water height needed at the bottom of the well for a water drawing vessel to function), minus the local offset between modern water table and sea level. For the local offset, since there are no continuous measurements in the archaeological wells apart from those measured previously in Caesarea (Sivan et al., 2004), two newly calculated modern offsets (Supplemental Table 1) were tested.

3.4.1 | Method A: average modern water table from coastal areas

For each of the ancient studied sites, averages of all water-table elevations measured by the Israeli Hydrological Survey for the last six decades were calculated (Table 2). As mentioned in the methods section above, average water-table elevation in each area represents the local modern offset between the coastal water table and modern sea level needed for calculating past RSL (see: "new offset A" in Supplemental Table 1). In Akko, the average offset was found to be half that of other sites along the Israeli coast which were in general almost the same, with the highest water-table elevations in Caesarea (Table 2). The unique hydrological condition in the Akko area, being located in a peninsula, could be responsible for its lower hydraulic gradient and lower water levels. To determine whether modern pumping activities do alter water-table offsets, we examined data from seven modern wells around Caesarea divided into decadal time-slices (Table 4).

3.4.2 | Method B: modeled elevations of coastal water table as a function of distance from present coastline

The average modern water-table elevations as a function of the distance from the coastline are displayed in Table 3. Figure 7 shows a plot of the wells using this offset.

4 | DISCUSSION

Very little sea-level research around the Mediterranean or elsewhere uses coastal wells as a tool for reconstructing ancient sea-level change. Though the method itself is not new in Israel, this study aims to provide the refinement necessary before wells can be used as a RSL indicator in other regions. Coastal underwater wells were used as sea-level indicators for the early Holocene (Galili et al., 1988; 2005) and along the coast of Israel either in scattered wells from different sites where the water-table elevation was estimated (Nir, 1997) or in many wells located in a smaller area ≤1 km^2 at 1st – 13th century CE Caesarea (Sivan et al., 2004). The Caesarea evaluated sea-level record is based on continuous measurements of the modern groundwater in the ancient wells. The current study uses data (wells bottom elevation and an age for the well-operating period) from coastal wells along the whole Israeli coast (from Ashdod-Yam in the south to Akko in the north, some 160 km apart) together with a modern offset. The most important part of the current study is its recommendations on evaluating the modern water-table offsets suitable to each site.

4.1 | Well bottom elevations

Though fresh water along the coast can exist down to a few tens of meters under the surface, humans dug wells as shallow as possible despite the need for fresh water all year round, because excavating in the coastal water table quickly becomes difficult, dangerous, and unnecessary. Wells dug in the friable sediments of the southern Levant such as unconsolidated sand or permeable sandstone rock need structural support (Nir, 1997; Figs. 2c and 2d) which becomes impossible as the well goes deeper and groundwater rises higher than ~0.5 m.

The measured elevations of the well bottoms vary through time but contain a relatively high degree of deviation even within one time period (Fig. 5). In Caesarea (Sivan et al., 2004), well bottoms show differences in elevations up to 0.60 m from *ca*. 400 – 700 CE. When a well at Yavne-Yam from the same period (Vunsh et al., 2014b) is added, the range grows to 0.85 m (Fig. 5). At Crusader Akko, the base elevations also differ substantially when measurements from different studies are combined (Fig. 5).

The base elevations in Caesarea are consistently higher than those in other areas (Fig. 5). This can be explained by a) different substrate: solid cemented calcareous sandstone in almost all sites except in Caesarea where the wells were excavated and built in the unconsolidated sand; and/or b) the local hydrological regime. The Caesarea aquifer has more recharge than other locations and a higher hydrological water level indicated in modern records (Table 2) (Dafny et al. 2010). As a result, it is probable the ancient population was able to dig shallower wells here.

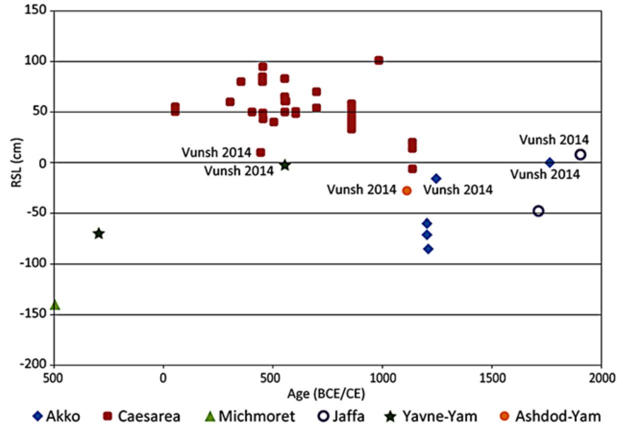

FIGURE 5 Water well bottom elevations from the past 2500 years at various sites in Israel [Color figure can be viewed at wileyonlinelibrary.com]

In Akko, Crusader water wells excavated for the current and prior studies (Nir, 1997; Toker et al., 2012) have the lowest bottoms (Fig. 5). Also in Caesarea, although the Crusader well bottoms are the highest relative to the Crusader bottoms in other sites, they are still the lowest relative to other periods. The low Crusader levels are corroborated by other types of archaeological indications found in Israel (for details see Toker et al., 2012).

4.2 | Calculating Israeli past RSL using coastal water wells

Since no long-term, continuous water-table measurements were carried out in the ancient wells, the current study sought other, more reliable methods for obtaining the offset between water table and sea level for the well transfer function. As mentioned in the methods section, two methods for calculating offset were tested; the first (offset A) is presented in Tables 2 and 4, the second (offset B) in Table 3 and Figure 6. Figure 7 shows a representation of wells using the numerical model offsets with ellipses representing 2σ uncertainties (following Hijma et al., 2015).

The results indicate that modern average water-table elevations are almost the same along most of the Israeli coast with slightly higher (4–14 cm) average levels in Caesarea, and significantly lower levels in Akko, where they were roughly half of levels found elsewhere (Table 2). The results of decadal time-slices of water-table elevations in Caesarea indicate that the elevations did not change much through the last few decades and therefore there are no indications of modern human influence (Table 4). These results strengthen the working assumption that modern offsets between sea level and the water table can be used for calculating past sea levels. RSL trends remain the same as those presented in Sivan et al. (2004) and in Toker et al. (2012) but the elevations change with the use of the new offsets. By using these calculations (offset A), the whole sea-level curve from Caesarea's continuous record is now lower by 0.26 m (Supplemental Table 1). This places the Roman–Byzantine maximum level at about +0.19 m rather than the

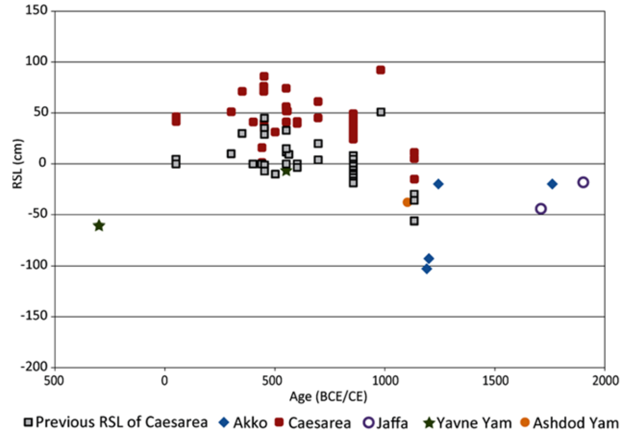

FIGURE 6 Newly calculated RSLs for the coast of Israel based on the modeled modern sea levels as a function of the distance from the coastline (offset B). The newly calculated RSLs of Nir (1997), Sivan et al. (2004) and Toker et al. (2012) are re-calculated based on the current suggested offset B and are compared to the new data obtained in our study [Color figure can be viewed at wileyonlinelibrary.com]

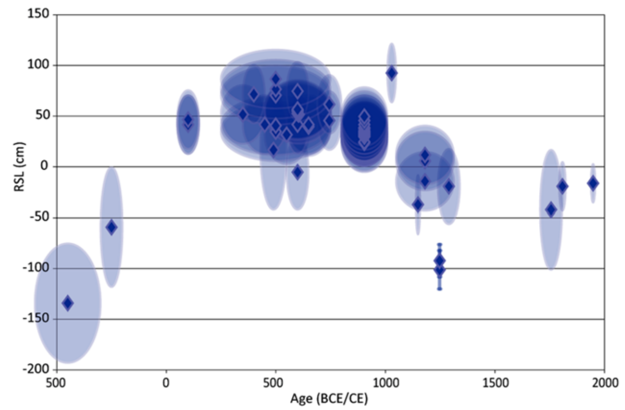

FIGURE 7 Offset B (Fig. 6. above) relative sea levels with chronological and vertical uncertainties represented as ellipses (approximates 2σ, following Hijma et al., 2015) [Color figure can be viewed at wileyonlinelibrary.com]

previously calculated +0.45 m. These new calculations are in agreement with other Mediterranean records (e.g., Anzidei et al., 2011). For the Crusader period, they are now as low as −0.82 m for Caesarea wells and −1.04 m when using a decadal average offset of 0.49 for Akko.

The modern wells used for calculating offset A are located between 20 and 200 m from the coastline. This is problematic since large differences in water level are expected over this distance. Therefore, we tested the second alternative: Fig. 6 presents the RSLs calculated by using offset B. In Caesarea, the new calculated RSLs (offset B) are slightly higher (and now reach elevations up to 74 cm) than the one calculated in Sivan et al. (2004).

In contrast to the Byzantine/Early Muslim period, in the Fatimid and Crusader periods (1000 – 1200 CE), sea levels were relatively low as previously concluded (Toker et al., 2012). The new dating and RSL (-0.38 m) for Ashdod-Yam is now in agreement with RSL reconstructions from Akko of −0.55 m (Nir, 1997) and the current study's results of −0.20 m from the ICC building well (Fig. 6).

Comparison of the current study's calculated sea levels with those derived from the fixed Vermetidae *Dendropoma petraeum* (Sivan et al., 2010) also confirms that around the 10th/11th century CE sea levels were already falling significantly. It is also in agreement with larger-scale sea-level data published by Kopp et al. (2016) indicating rise from 0 to 700 CE and fall between 1000 and 1400 CE based on statistical analysis of many datasets (including Sivan et al., 2004). It may be added that Toker et al. (2012) suggested driving mechanisms for the Crusader period low levels but no firm evidence has been provided thus far.

In the second half of the current millennium, the two wells from Jaffa (Fig. 6) match data obtained from bioconstructions (Sisma-Ventura et al., 2014) indicating slow rise of sea level from −0.43 m at the beginning of the 18th century to −0.17 m by 1900 CE.

5 | CONCLUSIONS

In the current study, five new index points were found reliable (based on their elevation measurements and dating) and were added to the Israeli dataset. All are from ancient water wells. Other secondary archaeological indicators – the cisterns and the water mills – are considered upper limiting sea-level data points. Base elevations of coastal wells differ in the same period. This is true for wells at the same site but disparities are even greater ($\leq$ 100 cm) between different sites. For this reason, we recommend consulting hydrological experts when calculating water-table offsets and calculating more conservative vertical errors for index points than the previously accepted $\pm$15 cm. In this study, we derived a more conservative error from the standard deviation of measured water-table offsets at the same distance from shore as the well. One of the more significant outcomes of our study is that the accuracy of coastal well SLIPs relies on finding the modern offset between water table and sea level; so high-resolution continuous monitoring of the water table at the archaeological site is crucial. Since such monitoring is usually not possible, we presented two alternatives: A) a long-term average of the groundwater levels measured by hydrological services near the site; and B) modeled groundwater levels derived from the distance of the ancient well to shore. Overall, for the Israeli coast, method B appears to be the most reliable, since it uses an estimated hydrological gradient based on simulations and actual field data from the Israeli coastal aquifer. These simulations show quite a large difference in the groundwater levels in the 200 m adjacent to the sea (0.63 m and 0.24 m at distances of 200 m and 20 m, respectively). Near-shore distances must be carefully measured since the hydraulic gradient is sharpest near the coastline.

The Israeli sea-level curve calculated in the current study using the new modeled offset shows trends identical to those previously reported. The Crusader (11th to 13th century CE) sea levels obtained by coastal water wells are always lowest relative to other periods, which confirm data from other archaeological and bioconstruction index points. With the current study's refinement and verification of ancient coastal water wells as reliable sea-level indicators, this class of archaeological remain has significant potential for reconstructing sea level in other areas of the Mediterranean.

ACKNOWLEDGEMENTS

The authors would like to thanks the two anonymous reviewers for their thoughtful comments. The authors are also indebted to the following individuals and bodies for providing assistance: Hatter family research grant and the ISF; Survey of Israel: Y. Meltzer, B. Shirman; Israel Antiquities Authority: U. Dahari, E. Stern, L. Rauchberger, N. Paran, M. Ajami, E. Hadad, D. Nachlieli, K. Refael, S. Sa'id and U. Ad; Israel National Parks Authority: T. Tzuk, A. Shahar; Hydrological Survey: L. Netzer; Tel Aviv University: M. Fischer; The Waqf of Akko; Restoration of Ancient Technology: Y. Dry; K. Yazdani (Bahai Community); Matta family; H. Abu al-Afia; M. Kaufman; N. Yoselevitz; and N. Yoselevitz for the graphics.

ORCID

Oren Tal http://orcid.org/0000-0002-7339-4851

REFERENCES

Antonioli, F., Ferranti, L., Fontana, A., Amorosi, A., Bondesan, A., Braitenberg, C., … Stocchi, P. (2009). Holocene relative sea-level changes and vertical movements along the Italian and Istrian coastlines. *Quaternary International*, *206*, 102–133.

Anzidei, M., Antonioli, F., Benini, A., Lambeck, K., Sivan, D., Serpelloni, E. & Stocchi, P. (2011). Sea-level change and vertical land movements since the last two millennia along the coasts of southwestern Turkey and Israel. *Quaternary International*, *232*, 13–20.

Anzidei, M., Lambeck, K., Antonioli, F., Furlani, S., Mastronuzzi, G., Serpelloni, E., & Vannucci, G. (2014). *Coastal structure, sea-level changes and vertical motion of the land in the Mediterranean. Geological Society*, London: Special Publications.

Arbel, Y., & Rauchberger, L. (2012). The Jerusalem Gate in Ottoman Jaffa in a rare photograph of Bonfils. *Et-Mol*, *216*, 16–18. (in Hebrew).

Auriemma, R., & Solinas, E. (2009). Archaeological remains as sea level change markers: A review. *Quaternary International*, *206*, 134–146.

Blackman, D. J. (1982). Ancient harbours in the Mediterranean. Part 1. *International Journal of Nautical Archaeology*, *11*, 79–104.

Blackman, D. J., Rankov, B., Baika, K., Gerding, H., & Pakkanen, J. (2014). *Shipsheds of the ancient Mediterranean*. Cambridge: Cambridge University Press.

Cocks, J. (2007). Historic Assessment International Conservation Center 175 Ha-Hagana Street Acre, Israel. Acre.

Dafny, E., Burg, A., & Gvirtzman, H. (2010). Effects of karst and geological structure on groundwater flow: the case of Yarqon-Taninim aquifer, Israel. *Journal of Hydrology*, *389*, 260–275.

Dean, S. (2015). 3,000 Years of East Mediterranean Sea Levels: Archaeological Indicators from Greece Combined with Israeli Coast Data. MA Thesis. Haifa: University of Haifa.

Diersch, H.-J. (2014). *Finite element modeling of flow, mass and heat transport in porous and fractured media*. Berlin & Heidelberg: Springer Science & Business Media.

Dray, Y. (2011). Flour-mills at the site of Tanninim Dam – variety of technologies. In A. Kidron & A. Izdarechet (Eds.), *Machmaney Caesarea: Summaries and Studies about Caesarea and its Surroundings.* Jerusalem: Friends of ancient Caesarea. (in Hebrew). (Vol. 1, pp. 141–158).

Flemming, N. C. (1968). Holocene earth movements and eustatic sea level change in the Peloponnese. *Nature*, *217*, 1031–1032.

Flemming, N. C., Raban, A. & Goetschel, C. (1978). *Tectonic and eustatic changes in the Mediterranean coast of Israel in the last 9000 years.* In J.C. Gamble & R.A. Yorke (Eds.), Progress in Underwater Science. Vol. 3 (New Series) of the report of the Underwater Association. Proceedings of the 11th Symposium at the British Museum (Natural History, 18–19th March, 1977 (pp. 33–93). London: Pentech Press.

Galili, E., & Weinstein-Evron, M. (1985). Prehistory and paleoenvironments of submerged sites along the Carmel coast of Israel. *Paléorient*, *11*(1), 37–52.

Galili, E., Weinstein-Evron, M. & Ronen, A. (1988). Holocene sea-level changes based on submerged archaeological sites off the northern Carmel coast in Israel. *Quaternary Research*, *29*, 36–42.

Galili, E., & Nir, Y. (1993). The submerged Pre-Pottery Neolithic water well of Atlit-Yam, northern Israel, and its palaeoenvironmental implications. *The Holocene*, *3*, 265–270.

Galili, E., Zviely, D. & Weinstein-Evron, M. (2005). Holocene sea-level changes and landscape evolution on the northern Carmel coast (Israel). *Mediterranée*, *1*(2), 1–8.

Galili, E., & Sharvit, J. (1998). Ancient coastal installations and the tectonic stability of the Israeli coast in historical times. In I.S. Stewart & C. Vita-Finzi (Eds.), *Coastal Tectonics, Geological Society* (Vol. 146, pp. 147–163). London: Special Publications.

Gleason, K. L., Burrell, B., Netzer E. & Taylor, L., Williams, J. H. (1998). The promontory palace at Caesarea Maritima: preliminary evidence for Herod's praetorium. *Journal of Roman Archaeology*, *11*, 23–52.

Hijma, M. P., Engelhart, S. E., Törnqvist, T. E., Horton, B. P., Hu, P. & Hill, D. F. (2015). In: I. Shennan, A.J. Long, B.P. Horton (Eds.), *Handbook of Sea-Level Research* (pp. 536–553). Oxford: John Wiley & Sons, Ltd.

Issar, A. (1968). Geology of the central Coastal Plain of Israel. *Israel Journal of Earth Sciences*, *17*, 16–29.

Kafri, U. (1967). Facies changes in southwestern Carmel (Israel) and their influence on groundwater regime. *Israel Journal of Earth Sciences*, *16*, 206–214.

Kafri, U. (1970). The cenomanian-turonian calcareous aquifer of central and western Galilee, Israel. *Bulletin of the International Association of Scientific Hydrology 15*, 77–91.

Kopp, R. E., Kemp, A. C., Bittermann, K., Horton, B. P., Donnelly, J. P., Gehrels, W. R., … Stefan Rahmstorf, S. (2016). Temperature-driven global sea-level variability in the common era. *PNAS*, *113*(11), E1434–E1441.

Kosmas, P., Kapsimalis, V., Theodorakopoulou, K. & Panagiotopoulos, I. P. (2012). Vertical displacement trends in the Aegean coastal zone (NE Mediterranean) during the Holocene assessed by geo-archaeological data. *The Holocene*, *22*, 717–728.

Lambeck, K. (1995). Late Pleistocene and Holocene sea-level change in Greece and south-western Turkey: a separation of eustatic, isostatic and tectonic contributions. *Geophysical Journal International*, *122*, 1022–1044.

Lambeck, K., & Bard, E. (2000). Sea-level change along the French Mediterranean coast for the past 30,000 years. *Earth and Planetary Science Letters*, *175*, 203–222.

Lambeck, K., Antonioli, F., Purcell, A., & Silenzi, S. (2004a). Sea-level change along the Italian coast for the past 10,000 yr. *Quaternary Science Reviews*, *23*, 1567–1598.

Lambeck, K., Anzidei, M., Antonioli, F., Benini, A., & Esposito, A. (2004b). Sea-level in Roman time in the Central Mediterranean and implications for recent change. *Earth and Planetary Science Letters*, *224*, 463–575.

Lambeck, K., & Purcell, A. (2005). Sea-level change in the Mediterranean Sea since the LGM: model predictions for tectonically stable areas. *Quaternary Science Reviews*, *24*, 1969–1988.

Lambeck, K., Antonioli, F., Anzidei, M., Ferranti, L., Leoni, G., Scicchitano, G., & Silenzi, S. (2011). Sea-level change along the Italian coast during the Holocene and projections for the future. *Quaternary International*, *232*, 250–257.

Levanon, E., Yechieli, Y., Shalev, E., Friedman, V., & Gvirtzman, H. (2013). Reliable monitoring of the transition zone between fresh and saline waters in coastal aquifers. *Groundwater Monitoring & Remediation*, *33*, 101–110.

Levanon, E., Yechieli, Y., Gvirtzman, H, & Shalev, E. (2017). Tide-induced fluctuations of salinity and groundwater level in unconfined aquifers – field measurements and numerical model. *Journal of Hydrology*, *551*, 665–675.

Lutzki, H., & Shalev, R., (2010). Slug Test for Measurements of Hydraulic Conductivity and Boreholes Intactness at the Coastal Plain Aquifer. Geological Survey of Israel Report. (in Hebrew).

Morhange, C., & Marriber, N. (2014). Archeological and biological relative sea-level indicators In I. Shennan, A.J. Long, B.P. Horton (Eds.), *Handbook of Sea-Level Research* (pp. 146–156). Oxford: Oxford University Press.

Morhange, C., Laborel, J., & Hesnard, A. (2001). Changes of relative sea-level during the past 5000 years in the ancient habour of Marseilles, Southern France. *Palaeogeography Palaeoclimatoogy Palaeoecology*, *166*, 319–329.

Morhange, C., Marriner, N., Excoffon, P., Bonnet, S., Flaux, C., Zibrowius, H., … Amouri, M. E. (2013). Relative sea-level changes during Roman times in the northwest Mediterranean: the 1st century AD fish tank of Forum Julii, Fréjus, France. *Geoarchaeology*, *28*, 363–372.

Murray-Wallace, C. V., & Woodroffe, C. D. (2014). *Quaternary sea-level changes: a global perspective*. Cambridge: Cambridge University Press.

Netzer, E. (1996). The promontory palace. In A. Raban & K.G. Holum (Eds.), *Caesarea Maritima: A Retrospective after Two Millennia* (pp. 193–207). Leiden: E.J. Brill.

Nielsen, P. (1990). Tidal dynamics of the water table in beaches beach. *Water Resources Research*, *26*, 2127–2134.

Nir, Y. (1997). Middle and late Holocene sea-level along the Israeli Mediterranean coast: evidence from ancient water wells. *Journal of Quaternary Science*, *12*, 143–151.

Nir Y., & Eldar, I. (1986). Ancient Ground-Water Table in Old Wells as an Indicator of Paleo Sea-Levels and Neotectonic Changes along the Coastal Plain of Israel. Geological Survey of Israel Report. (in Hebrew).

Pirazzoli, P. A. (1976). Sea-level variations in the northwest Mediterranean during Roman times. *Science*, *194*, 519–521.

Pirazzoli, P. A. (1991). *World Atlas of Holocene Sea-Level Changes*. Amsterdam: Elsevier Science Publishers.

Porat, N., Sivan, D., & Zviely, D. (2008). Late Holocene embayment infill and shoreline migration, Haifa Bay, Eastern Mediterranean. Israel. *Journal of Earth Sciences*, *57*, 21–31.

Pugh, D. T. (1996). *Tides, purges and mean sea level*. Chichester, UK: John Wiley & Sons Ltd.

Raban, A. (1983). Recent maritime archaeological research in Israel. *International Journal of Nautical Archaeology*, *12*, 229–251.

Raban, A. (1995). Dor-Yam: Marine and coastal installations at Dor in their geomorphological and stratigraphic context. In: Stern, E., (Director), *Excavations at Dor, Final Report Volume 1A, Areas A and C, Introduction and Stratigraphy* (Qedem Reports 1A). Institute of Archaeology, The Hebrew University of Jerusalem and the Israel Exploration Society, Jerusalem, 285–354.

Raban, A., & Galili, E. (1985). Recent maritime archaeological in Israel: A preliminary report. *International Journal of Nautical Archaeology*, *14*, 321–356.

Raphael, S. K. (2014). Azdud (Ashdod-Yam): an early Islamic fortress on the Mediterranean coast. *Bar International Series 2673*, Oxford: Archaeopress.

Sa'id, A. S. (2002). Nahal Tanninim dam. *Ḥadashot Arkheologiyot—Excavations and Surveys in Israel*, *114*, 38.

Sa'id, A. S., & 'Ad, U. (2004). Nahal Tanninim dam. *Ḥadashot Arkheologiyot—Excavations and Surveys in Israel*, *116*. Retrieved from http://www.hadashot-esi.org.il/Report_Detail_Eng.aspx?id=11&mag_id=108

Shennan, I. (2014). Handbook of sea-level research: framing research questions (pp. 3(28). In I. Shennan, A.J. Long & B.P. Horton (Eds.), *Handbook of Sea-Level Research*. Oxford: Oxford University Press.

Sisma-Ventura, G., Yam, R., & Shemesh, A. (2014). Recent unprecedented warming and oligotrophy of the eastern Mediterranean Sea within the last millennium. *Geophysical Research Letters*, *41*(14), 5158–5166.

Sivan, D., Wdowinski, S., Lambeck, K., Galili, E., & Raban, A. (2001). Holocene sea-level changes along the Mediterranean coast of Israel, based on archaeological observations and numerical model. *Palaeogeography, Palaeoclimatology, Palaeoecology*, *167*, 101–117.

Sivan, D., Lambeck, K., Toueg, R., Raban, A., Porath, Y., & Shirnam, B. (2004). Ancient coastal wells of Caesarea Maritima, Israel, an indicator for relative sea-level changes during the last 2000 years. *Earth and Planetary Science Letters*, *222*(1), 315–330.

Sivan, D., Schattner, U., Morhange, C., & Boaretto, E. (2010). What can a sessile mollusk tell about the neotectonics. *Earth and Planetary Science Letters*, *296*(3–4), 451–458.

Sneh, Y., & Klein, M. (1984). Holocene sea-level changes at the coast of Dor, southeast Mediterranean. *Science*, *226*, 831–832.

Stocchi, P., & Spada, G. (2009). Influence of glacial isostatic adjustment upon current sea level variations in the Mediterranean. *Tectonophysics*, *474*(1–2), 56–68.

Tal, O., & Taxel, I. (2012). Socio-political and economic aspects of refuse disposal in late Byzantine and early Islamic Palestine (pp. 497–518). In R. Matthews, J. Curtis (Eds.), *Proceedings of the 7th International Congress on the Archaeology of the Ancient Near East, 12–16, April 2010*. Wiesbaden: Otto Harrassowitz GmbH & Co.

Toker, E., Sivan, D., Stern, E., Shirman, B., Tsimplis, M., & Spada, G. (2012). Evidence for centennial scale sea-level variability during the Medieval Climate Optimum (Crusader Period) in Israel, eastern Mediterranean. *Earth Planetary Science Letters*, 315–316, 51–61.

Vacchi, M., Rovere, A., Chatzipetros, A., Zouros, N., & Firpo, M. (2014). An updated database of Holocene relative sea-level changes in NE Aegean Sea. *Quaternary International*, 328–329, 301–310.

Vacchi, M., Marriner, N., Morhange, C., Spada, G., Fontana, A., & Rovere, A. (2016). Multiproxy assessment of Holocene relative sea-level changes in the western Mediterranean: Sea-level variability and improvements in the definition of the isostatic signal. *Earth Science Reviews*, *155*, 172–197.

Vött, A. (2007). Relative sea level changes and regional tectonic evolution of seven coastal areas in NW Greece since the mid-Holocene. *Quaternary Science Reviews*, *26*, 894–919.

Vunsh, R. (2014). East Mediterranean Late Holocene Relative Sea-Level Changes Based on Archaeological Indicators from the Coast of Israel. MA Thesis. Haifa: University of Haifa. (in Hebrew).

Vunsh, R., Tal, O., & Sivan, D. (2013). Ḥorbat Ashdod-Yam. *Ḥadashot Arkheologiyot—Excavations and Surveys in Israel*, *125*. Retrieved from http://www.hadashot-esi.org.il/report_detail_eng.aspx?id=2294&mag_id=120.

Vunsh, R., Tal, O., & Sivan, D. (2014a). Yafo, Yefet street. *Ḥadashot Arkheologiyot—Excavations and Surveys in Israel*, *126*. Retrieved from http://www.hadashot-esi.org.il/report_detail_eng.aspx?id=8530&mag_id=121.

Vunsh, R., Tal, O., Sivan, D., & Fischer, M. (2014b). Yavne-Yam. *Ḥadashot Arkheologiyot—Excavations and Surveys in Israel*, *126*. Retrieved from http://www.hadashot-esi.org.il/report_detail_eng.aspx?id=7483&mag_id=121.

Zach, S. (2007). The work on two column bases at the ICC building, Old Akko. Final project for the International Conservation Center. Acre.

SUPPORTING INFORMATION

Additional Supporting Information may be found online in the supporting information tab for this article.

How to cite this article: Vunsh R, Tal O, Yechieli Y, Dean S, Levanon E, Sivan D. Evaluating ancient coastal wells as sea-level indicators from the coast of Israel. *Geoarchaeology*. 2018;33:403–416. https://doi.org/10.1002/gea.21663

Supplemental Table 1: The Israeli coastal water wells: sites, base elevations and water table offsets used for calculating past sea level: previously published offsets (offset A), based on average water table elevations in the last few decades and the modeled modern water table elevation (offset B) as a function of the distance from the coastline (the calculations use the function determined by Sivan et al., 2004).

ID	Site	Site feature	Well base (cm)	Date	Date uncertainty	Previous offset	Previous RSL (cm)	New offset A (cm)	New RSL (A)	Distance from coastline (m)	New offset B (cm)	New RSL (B)	RSL vertical uncertainty	References
4	Akko	Well base	-85	1205 CE	7	18	-73	49	-104					Nir 1997
5	Akko	well bottom, Hospitaller room	-71	1199 CE	5	18	-59	49	-90	185	61	-102	19	Unpublished data
6	Akko	well bottom, Hospitaller compound	-60	1199 CE	5	18	-48	49	-79	200	63	-93	16	Toker et al., 2012
7	Akko	well bottom, 36/11 St well	0	1760 CE	15	18	12	49	-19	120	50	-20	24	Vunsh 2014
8	Akko	well bottom, ICC building	-16	1241 CE	50	18	-4	49	-35	50	34	-20	37	Vunsh 2014
10	Michmoret	well bottom	-140	500 BCE	150					30	25	-135	59	Nir 1997; Sivan et al., 2001
19	Caesarea	well bottom	55	50 CE	50	80	5	106	-21	70	39	46	29	Sivan et al., 2004
20	Caesarea	well bottom	50	50 CE	50	80	0	106	-26	70	39	41	29	Sivan et al., 2004
21	Caesarea	well bottom	50	50 CE	50	80	0	106	-26	70	39	41	29	Sivan et al., 2004
22	Caesarea	well bottom	60	300 CE	100	80	10	106	-16	70	39	51	29	Sivan et al., 2004
23	Caesarea	well bottom	80	350 CE	50	80	30	106	4	70	39	71	29	Sivan et al., 2004
24	Caesarea	well bottom	50	400 CE	100	80	0	106	-26	70	39	41	29	Sivan et al., 2004
25	Caesarea	well bottom	40	500 CE	100	80	-10	106	-36	70	39	31	29	Sivan et al., 2004
26	Caesarea	well bottom	65	550 CE	150	80	15	106	-11	70	39	56	29	Sivan et al., 2004
27	Caesarea	well bottom	61	550 CE	150	80	11	106	-15	70	39	52	29	Sivan et al., 2004
28	Caesarea	well bottom	63	550 CE	150	80	13	106	-13	70	39	54	29	Sivan et al., 2004
29	Caesarea	well bottom	64	550 CE	150	80	14	106	-12	70	39	55	29	Sivan et al., 2004
30	Caesarea	well bottom	60	555 CE	150	80	10	106	-16	70	39	51	29	Sivan et al., 2004
31	Caesarea	well bottom	83	550 CE	50	80	33	106	7	70	39	74	29	Sivan et al., 2004
32	Caesarea	well bottom	50	550 CE	50	80	0	106	-26	70	39	41	29	Sivan et al., 2004
33	Caesarea	well bottom	48	600 CE	100	80	-2	106	-28	70	39	39	29	Sivan et al., 2004
34	Caesarea	well bottom	50	600 CE	100	80	0	106	-26	70	39	41	29	Sivan et al., 2004

35	Caesarea	well bottom	49	450 CE	250	80	-1	106	-27	70	39	40	29	Sivan et al., 2004
36	Caesarea	well bottom	43	450 CE	250	80	-7	106	-33	70	39	34	29	Sivan et al., 2004
37	Caesarea	well bottom	79	450 CE	250	80	29	106	3	70	39	70	29	Sivan et al., 2004
38	Caesarea	well bottom	85	450 CE	250	80	35	106	9	70	39	76	29	Sivan et al., 2004
39	Caesarea	well bottom	95	450 CE	250	80	45	106	19	70	39	86	29	Sivan et al., 2004
40	Caesarea	well bottom	70	695 CE	55	80	20	106	-6	70	39	61	29	Sivan et al., 2004
41	Caesarea	well bottom	54	695 CE	55	80	4	106	-22	70	39	45	29	Sivan et al., 2004
42	Caesarea	well bottom	41	855 CE	105	80	-9	106	-35	70	39	32	29	Sivan et al., 2004
43	Caesarea	well bottom	32	855 CE	105	80	-18	106	-44	70	39	23	29	Sivan et al., 2004
44	Caesarea	well bottom	42	855 CE	105	80	-8	106	-34	70	39	33	29	Sivan et al., 2004
45	Caesarea	well bottom	47	855 CE	105	80	-3	106	-29	70	39	38	29	Sivan et al., 2004
46	Caesarea	well bottom	40	855 CE	105	80	-10	106	-36	70	39	31	29	Sivan et al., 2004
47	Caesarea	well bottom	42	855 CE	105	80	-8	106	-34	70	39	33	29	Sivan et al., 2004
48	Caesarea	well bottom	38	855 CE	105	80	-12	106	-38	70	39	29	29	Sivan et al., 2004
49	Caesarea	well bottom	50	855 CE	105	80	0	106	-26	70	39	41	29	Sivan et al., 2004
50	Caesarea	well bottom	38	855 CE	105	80	-12	106	-38	70	39	29	29	Sivan et al., 2004
51	Caesarea	well bottom	58	855 CE	105	80	8	106	-18	70	39	49	29	Sivan et al., 2004
52	Caesarea	well bottom	43	855 CE	105	80	-7	106	-33	70	39	34	29	Sivan et al., 2004
53	Caesarea	well bottom	38	855 CE	105	80	-12	106	-38	70	39	29	29	Sivan et al., 2004
54	Caesarea	well bottom	33	855 CE	105	80	-17	106	-43	70	39	24	29	Sivan et al., 2004
55	Caesarea	well bottom	54	855 CE	105	80	4	106	-22	70	39	45	29	Sivan et al., 2004
56	Caesarea	well bottom	43	855 CE	105	80	-7	106	-33	70	39	34	29	Sivan et al., 2004
57	Caesarea	well bottom	43	855 CE	105	80	-7	106	-33	70	39	34	29	Sivan et al., 2004
58	Caesarea	well bottom	41	855 CE	105	80	-9	106	-35	70	39	32	29	Sivan et al., 2004
59	Caesarea	well bottom	40	855 CE	105	80	-10	106	-36	70	39	31	29	Sivan et al., 2004
60	Caesarea	well bottom	38	855 CE	105	80	-12	106	-38	70	39	29	29	Sivan et al., 2004
61	Caesarea	well bottom	40	855 CE	105	80	-10	106	-36	70	39	31	29	Sivan et al., 2004
62	Caesarea	well bottom	42	855 CE	105	80	-8	106	-34	70	39	33	29	Sivan et al., 2004
63	Caesarea	well bottom	40	855 CE	105	80	-10	106	-36	70	39	31	29	Sivan et al., 2004
64	Caesarea	well bottom	43	855 CE	105	80	-7	106	-33	70	39	34	29	Sivan et al., 2004
65	Caesarea	well bottom	46	855 CE	105	80	-4	106	-30	70	39	37	29	Sivan et al., 2004
66	Caesarea	well bottom	44	855 CE	105	80	-6	106	-32	70	39	35	29	Sivan et al., 2004
67	Caesarea	well bottom	50	855 CE	105	80	0	106	-26	70	39	41	29	Sivan et al., 2004
68	Caesarea	well bottom	43	855 CE	105	80	-7	106	-33	70	39	34	29	Sivan et al., 2004

69	Caesarea	well bottom	40	855 CE	105	80	-10	106	-36	70	39	31	29	Sivan et al., 2004
70	Caesarea	well bottom	41	855 CE	105	80	-9	106	-35	70	39	32	29	Sivan et al., 2004
71	Caesarea	well bottom	43	855 CE	105	80	-7	106	-33	70	39	34	29	Sivan et al., 2004
72	Caesarea	well bottom	39	855 CE	105	80	-11	106	-37	70	39	30	29	Sivan et al., 2004
73	Caesarea	well bottom	41	855 CE	105	80	-9	106	-35	70	39	32	29	Sivan et al., 2004
74	Caesarea	well bottom	40	855 CE	105	80	-10	106	-36	70	39	31	29	Sivan et al., 2004
75	Caesarea	well bottom	41	855 CE	105	80	-9	106	-35	70	39	32	29	Sivan et al., 2004
76	Caesarea	well bottom	42	855 CE	105	80	-8	106	-34	70	39	33	29	Sivan et al., 2004
77	Caesarea	well bottom	43	855 CE	105	80	-7	106	-33	70	39	34	29	Sivan et al., 2004
78	Caesarea	well bottom	40	855 CE	105	80	-10	106	-36	70	39	31	29	Sivan et al., 2004
79	Caesarea	well bottom	101	980 CE	20	80	51	106	25	70	39	92	29	Sivan et al., 2004
80	Caesarea	well bottom	-6	1133 CE	132.5	80	-56	106	-82	70	39	-15	29	Sivan et al., 2004
81	Caesarea	well bottom	14	1133 CE	132.5	80	-36	106	-62	70	39	5	29	Sivan et al., 2004
82	Caesarea	well bottom	20	1133 CE	132.5	80	-30	106	-56	70	39	11	29	Sivan et al., 2004
83	Caesarea	well bottom	10	440 CE	60	80		106	-66	20	24	16	59	Gleason et al., 1998
84	Jaffa	Base of Abu al-Afia well	8	1900 CE	10			97	-59	150	55	-17	19	Vunsh et al., 2014b
85	Jaffa	Base of M. Kaufman well	-48	1708 CE	50	11	-29	97	-115	25	25	-43	59	Toker et al., 2012
86	Yavne-Yam	well bottom	-70	300 BCE	50				-40	15	20	-60	59	Nir and Eldar 1986; Nir 1997; Sivan et al., 2001
87	Yavne-Yam	Base of well relative to MSL	-2	550 CE	50			98	-70	50	34	-6	37	Vunsh ey al., 2014a
88	Ashdod-Yam	Base of well relative to MSL	-28	1100 CE	10			92	-90	80	40	-38	29	Vunsh et al., 2013
89	Ashqelon	well bottom		5 CE	68		0							Nir 1997
90	Ashqelon	well bottom		5 CE	68		0							Nir 1997
91	Ashqelon	well bottom		480 CE	157		0							Nir 1997
92	Ashqelon	well bottom		230 CE	94		0							Nir 1997
93	Ashqelon	well bottom		480 CE	157		0							Nir 1997
94	Ashqelon	well bottom		480 CE	157		-20							Nir 1997